Discreet protein networks mediate age-related loss of large dendritic spines in the precuneus

Krivinko JM[1], Sui Z[2], Happe C[1], Hensler C[1], McKinney BC[1], Newman J[1], Ding Y[2], MacDonald ML[1], Sweet RA[1,3]

[1]Department of Psychiatry and [3]Department of Neurology, University of Pittsburgh School of Medicine, Pittsburgh, PA
[2]Department of Biostatistics, University of Pittsburgh School of Public Health, Pittsburgh, PA

Background

- Loss of dendritic spine density in neocortical areas is closely correlated with cognitive decline in Alzheimer Disease (AD) (1). Preservation of dendritic spine density despite accumulation of AD-related pathology is associated with cognitive resilience (2).
- Previous reports have documented that increased age is itself correlated with loss of dendritic spine density in prefrontal cortex (3). However, upstream drivers of age-related dendritic spine loss are poorly understood.
- The precuneus, an area of the brain which accumulates AD-related pathology early in disease progression (4) and, when atrophied, consistently predicts conversion of mild cognitive impairment to AD (5), is an important area for detecting markers of risk and resilience to dementia onset. However, age-related alterations in dendritic spine density within the precuneus remain largely unstudied.
- We therefore undertook to determine the effect of age on dendritic spine density within the precuneus and identify protein mediators of age-related dendritic spine density alterations.

Materials and Methods

Subject demographics and neuropathology assessment

Brain tissue was obtained from 98 subjects at autopsy (Allegheny County Medical Examiner's Office, Pittsburgh, PA) following acquisition of informed consent from next of kin and in accordance with University of Pittsburgh's Committee for Oversight in Research Involving Decedents and the IRB for Biomedical Research. Consensus diagnoses, or lack thereof, were generated by a committee of experienced clinicians according to the DSM-IV. No subject had a documented diagnosis of a neurocognitive disorder. Subjects were evaluated at autopsy with sections from the frontal pole, hippocampus, entorhinal cortex, and cerebellum stained using H&E, Bielschowsky's stain, and amyloid β immunohistochemistry. No subject had sufficient evidence for a neurodegenerative disease. The median age of the cohort was 51 (range 20-96 years).

Age Group	N	Mean age, years	Sex, % female	Race, % black	Mean PMI, hours [SD]	Mean storage time, months [SD]	Age-appropriate path*, number (+) subjects	Leading cause of death (% affected)
20s	16	25.1	31.3	37.5	15.0 [6.6]	151.5 [76.3]	0[A]	Trauma (37.5)
30s	16	36.0	43.8	31.3	16.7 [7.1]	137.9 [67.0]	1[A]	Cardiovascular disease (37.5)
40s	16	44.7	50.0	43.4	15.6 [3.1]	144.1 [69.2]	2[B]	Cardiovascular disease (62.5)
50s	16	55.3	43.8	43.4	15.2 [3.3]	137.8 [69.6]	1[A]	Cardiovascular disease (62.5)
60s	16	64.3	50.0	31.3	15.2 [6.1]	173.6 [85.9]	1[C]	Cardiovascular disease (43.8)
>70	18	77.6	38.9	11.1	18.8 [5.6]	167.8 [62.9]	7[B]	Trauma (44.4)

Table 1. Subject demographics by age group. For each age bracket, demographics and the number of subjects found to have age-appropriate neuropathology are shown. *Age-appropriate neuropathology is defined as extracellular amyloid plaques, amyloid angiopathy, or neurofibrillary tangles present at levels not considered out of proportion for age according to an expert neuropathologist at time of autopsy. Footnotes: [A]neuropathology results unavailable for 1 subject, [B]neuropathology results unavailable for 2 subjects, [C]neuropathology results unavailable for 4 subjects

Tissue collection, quantitative immunohistochemistry, and confocal microscopy

The right precuneus was identified using the following boarders: marginal branch of the cingulate sulcus (anterior), subparietal sulcus (inferior), and parietooccipital sulcus (posterior). Two sections from each subject were slide mounted, fixed in 4% paraformaldehyde, permeabilized with 0.3% Triton-X in phosphate buffered saline (PBS), and incubated in 20% normal goat serum (NGS), 20% normal human serum (NHS), 1% bovine serum albumin (BSA), 0.1% glycine, and 0.1% lysine in PBS. Sections were incubated in 5% NGS, 5% NHS, 1% BSA, 0.1% glycine, and 0.1% lysine in PBS with spinophilin antibody (1:1500) for 24 hours at 4°C, rinsed in PBS, incubated with Alexa Fluor 488 antibody (1:500) and 3 units/μL Alexa Fluor 568 phalloidin, washed in PBS, and cover-slipped. Dendritic spines were visualized by colocalization of spinophilin and actin by phalloidin as previously described (6). Image stacks underwent blind deconvolution and gaussian subtraction prior to data segmentation. The intensity threshold for iterative segmentation for each channel was calculated using the Otsu iterative thresholding algorithm (7). Object masks were size gated after each iteration as previously described (8) and dendritic spines were defined as a ≥1 voxel overlap of a phalloidin masked object with a spinophilin masked object. Dendritic spines were categorized into three size categories: small (<0.45 um^3), medium (0.45-0.90 um^3), large (>0.90 um^3).

Tandem mass tag (TMT) mass spectrometry

Samples were coded and randomly assigned to one of eight plexes using a balanced block design. A global internal standard (GIS) which included a small aliquot from each homogenate and synaptosome sample, was added to each TMT plex. 30 mg of tissue was homogenized with a Dounce homogenizer in 300μL Syn-Per reagent (ThermoScientific) with protease and phosphatase inhibitors. 25μL of homogenate was added to an equal volume of S-trap buffer to generate the homogenate fraction; the remaining homogenate underwent a series of centrifugations, the pellet isolated and resuspended in 0.1mM $CaCl_2$ with protease and phosphatase inhibitors, centrifuged, and the pellet isolated and resuspended in S-trap buffer to generate the synaptosome fraction. Samples were bath sonicated, underwent protein quantification with micro-bicinchoninic acid assay, reduced with dithiothreitol, alkylated with iodoacetamide, acidified with phosphoric acid, and diluted six-fold in binding buffer. Samples were dispensed onto S-trap columns, incubated at 47°C in 50mM TEAB for trypsin digestion (1:10 enzyme/substrate), eluted, dried, resuspended in 100mM TEAB, and labeled with TMTpro™ 16. Samples were pooled into plexes which were fractionated using Pierce High pH Reversed-Phase Peptide Spin Columns (Thermo). Peptides were eluted into 9 fractions of increasing ACN concentrations, dried, and resuspended in 3% ACN and 0.1% formic acid to a final concentration of 0.5 μg/μL. Data were collected using an Orbitrap Eclipse Tribrid Mass Spectrometer and UltiMate 3000 UHPLC (ThermoFisher Scientific). Ions for MS3 were selected using real time search. Initial analysis was carried out in Proteome Discoverer and MS/MS spectra were searched against the human SwissProt database using Sequest-HT. Peptide spectral matches were filtered using Percolator with a dCN = 0.05 and FDR of 1%.

Bioinformatics and statistical analysis

The mean dendritic spine density for each spine size category for each subject was calculated and correlated with each subject's age using linear regression. Peptides were rolled up to protein using inverse-CV-weighted average of scaled peptide values. The effect of age on protein abundance was evaluated with multivariate linear regression with age as the predictor, sex, race, PMI, storage time and plex as covariates, and protein abundance as the outcome. Weighted Gene Correlation Network Analysis (WGCNA) (9) was conducted to generate protein co-expression modules. A mediation analysis (see schematic to the right) controlling for sex, race, PMI and IHC assay group was conducted to detect modules which mediated the effect of age on the density of large dendritic spines.

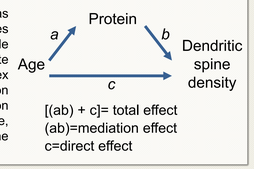

[(ab) + c]= total effect
(ab)=mediation effect
c=direct effect

Results

Figure 1—*The density of large dendritic spines declines with age in the precuneus*

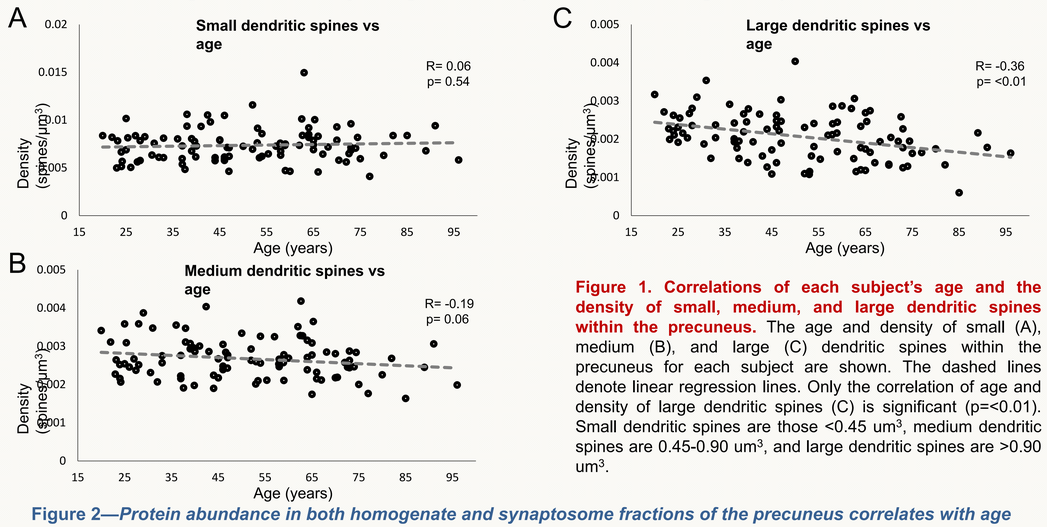

Figure 1. Correlations of each subject's age and the density of small, medium, and large dendritic spines within the precuneus. The age and density of small (A), medium (B), and large (C) dendritic spines within the precuneus for each subject are shown. The dashed lines denote linear regression lines. Only the correlation of age and density of large dendritic spines (C) is significant (p=<0.01). Small dendritic spines are those <0.45 um^3, medium dendritic spines are 0.45-0.90 um^3, and large dendritic spines are >0.90 um^3.

Figure 2—*Protein abundance in both homogenate and synaptosome fractions of the precuneus correlates with age*

Figure 2. Correlations of age and protein abundance within homogenate and synaptosome fractions. The regression coefficients and regression p values on a -log_{10} scale for each protein in homogenate (A) and synaptosome (B) is shown. The horizontal dashed line denotes the false discovery threshold (q value=<0.05); points above the dashed line denote proteins whose abundance levels are significantly correlated with age. 1839/5032 proteins detected in homogenate and 914/4754 proteins detected in the synaptosome fraction were significantly correlated with age after adjustment for false discovery.

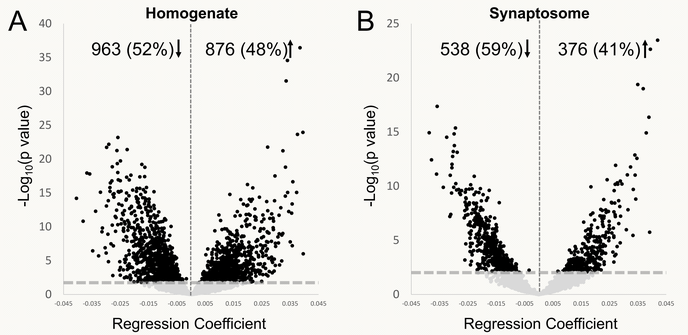

Figure 3—*Discreet protein networks statistically mediate the effect of age on the density of large dendritic spines*

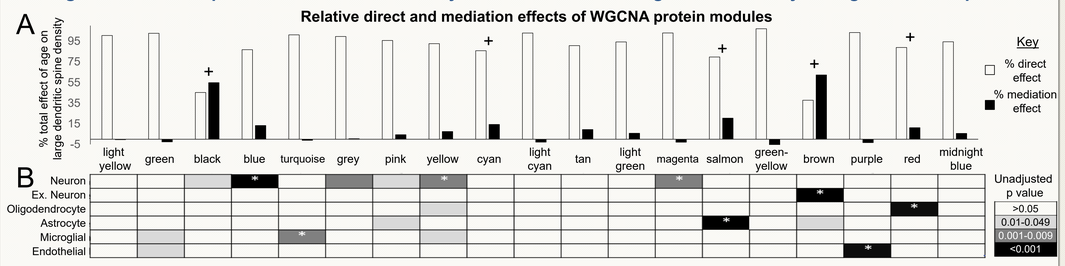

Figure 3. Cell type enrichment analysis and the relative contributions of the direct and mediation effects for each WGCNA protein module to the total effect of age on the density of large dendritic spines. (A) For each module assembled by WGCNA (9), the percent contributions of the direct age effect and the mediation effect to the total effect of age on large dendritic spine density are shown. The outcome variable is the density of large dendritic spines, the direct age effect is the effect of age after accounting for the effect of the module, the mediation effect is the effect of age mediated by the module, and the total effect is the sum of the direct and mediation effects (a constant). Modules which significantly mediate the effect of age on dendritic spine density are denoted by +. (B) Each protein module was evaluated for cell type enrichment in WebGestalt (10). Modules for which unadjusted cellular enrichment p values are less than 0.05 are denoted by shading, with lower p values indicated by higher grayscale saturation. Modules which contained significant cell type enrichment after adjustment for false discovery are denoted by white *.

Results (continued)

Table 2—*Protein modules which mediate the effect of age on the density of large dendritic spines contain unique functional enrichments*

Module	Gene ontology	Description	Number of genes	Enrich-ment Ratio	Unadjusted p value	Adjusted p value
BLACK	GO:2000463	positive regulation of excitatory postsynaptic potential	17	11.0	$6.02x10^{-05}$	0.034
	GO:0098815	modulation of excitatory postsynaptic potential	22	10.2	$1.7x10^{-05}$	0.014
	GO:0050803	regulation of synapse structure or activity	117	3.84	$5.56x10^{-05}$	0.034
	GO:0050804	modulation of chemical synaptic transmission	243	3.08	$5.05x10^{-06}$	0.014
	GO:0099177	regulation of trans-synaptic signaling	244	3.07	$5.38x10^{-06}$	0.014
BROWN	GO:0006836	neurotransmitter transport	151	3.91	$1.12x10^{-07}$	$3.18x10^{-4}$
	GO:0001505	regulation of neurotransmitter levels	181	3.75	$2.54x10^{-08}$	$1.44x10^{-4}$
	GO:0099537	trans-synaptic signaling	354	2.42	$5.32x10^{-06}$	0.004
	GO:0099536	synaptic signaling	357	2.40	$6.3x10^{-06}$	0.004
	GO:0030154	cell differentiation	1112	1.65	$9.08x10^{-06}$	0.005
RED	GO:0022010	myelination	9	21.47	$1.24x10^{-06}$	$6.39x10^{-4}$
	GO:0014003	oligodendrocyte development	20	13.53	$3.84x10^{-07}$	$3.11x10^{-4}$
	GO:0007272	ensheathment of neurons	61	8.87	$2.31x10^{-10}$	$4.37x10^{-7}$
	GO:0008366	axon ensheathment	61	8.87	$2.31x10^{-10}$	$4.37x10^{-7}$
	GO:0042552	myelination	61	8.87	$2.31x10^{-10}$	$4.37x10^{-7}$

Table 2. Gene ontology enrichment terms for modules which mediate the effect of age on large dendritic spine density. The gene ontology terms with the top five enrichment ratios for each module which statistically mediated the effect of age on the density of large dendritic spines are shown. Only terms which are significant after adjustment for false discovery are shown. The cyan and salmon modules failed to contain significant gene ontology term enrichment after adjustment for false discovery and are therefore not included. Enrichments were generated in WebGestalt (10) by evaluating for gene ontology term enrichment of the protein identities from each module relative to all proteins detected in homogenate, rather than relative to the entire genome, to increase stringency.

Conclusions & Future Directions

- The density of large, but not small or medium, dendritic spines was negatively correlated with age in the precuneus.
- Within the precuneus, the abundance of >1/3 of proteins detected in cellular homogenate were correlated with age, while <1/5 of proteins detected in the synaptosome fraction demonstrated significant age correlations.
- Five protein modules statistically mediated the effect of age on the density of large dendritic spines in the precuneus and were enriched for gene ontology terms related to regulation of EPSPs, neurotransmitter regulation, and myelination.
- Future studies employing reverse computational pharmacology may be useful to identify existing compounds which target protein mediators of age-related dendritic spine loss to enhance cognitive resilience to AD-related pathologies and protect against dementia onset.

Works Cited

1. Herms J and Dorostkar MM, Dendritic Spine Pathology in Neurodegenerative Diseases. Annu Rev Pathol, 2016. 11: p. 221-50.
2. Boros BD, Greathouse KM, Gentry EG, Curtis KA, Birchall EL, Gearing M, et al., Dendritic spines provide cognitive resilience against Alzheimer's disease. Ann Neurol, 2017. 82(4): p. 602-614.
3. Dickstein DL, Weaver CM, Luebke JI, and Hof PR, Dendritic spine changes associated with normal aging. Neuroscience, 2013. 251: p. 21-32.
4. Aghakhanyan G, Vergallo A, Gennaro M, Mazzarri S, Guidoccio F, Radicchi C, et al., The Precuneus - A Witness for Excessive Abeta Gathering in Alzheimer's Disease Pathology. Neurodegener Dis, 2018. 18(5-6): p. 302-309.
5. Jacobs HI, Van Boxtel MP, Jolles J, Verhey FR, and Uylings HB, Parietal cortex matters in Alzheimer's disease: an overview of structural, functional and metabolic findings. Neurosci Biobehav Rev, 2012. 36(1): p. 297-309.
6. MacDonald ML, Alhassan J, Newman JT, Richard M, Gu H, Kelly RM, et al., Selective Loss of Smaller Spines in Schizophrenia. Am J Psychiatry, 2017. 174(6): p. 586-594.
7. Otsu N, A Threshold Selection Method from Gray-Level Histograms. IEEE Transactions on Systems, Man, and Cybernetics, 1979. 9(1): p. 62-66.
8. McKinney BC, MacDonald ML, Newman JT, Shelton MA, DeGiosio RA, Kelly RM, et al., Density of small dendritic spines and microtubule-associated-protein-2 immunoreactivity in the primary auditory cortex of subjects with schizophrenia. Neuropsychopharmacology, 2019. 44(6): p. 1055-1061.
9. Langfelder P and Horvath S, WGCNA: an R package for weighted correlation network analysis. BMC Bioinformatics, 2008. 9: p. 559.
10. Zhang B, Kirov S, and Snoddy J, WebGestalt: an integrated system for exploring gene sets in various biological contexts. Nucleic Acids Res, 2005. 33(Web Server issue): p. W741-8.

Acknowledgements

The University of Pittsburgh holds a Physician-Scientist Institutional Award from the Burroughs Wellcome Fund (JMK). This work was supported by NIH grant MH116046 (RAS) and by a grant from the UPMC Immune Transplant and Therapy Center (ITTC).